DOI: 10.1002/ange.201208630

Peptoid Foldamers

A Peptoid Ribbon Secondary Structure**

*J. Aaron Crapster, Ilia A. Guzei, and Helen E. Blackwell**

Delineating the relationships between sequence, structure, and function in biopolymers is critical to our understanding of fundamental biochemical interactions. These relationships are equally important for the design of functional biomimetic oligomers (that is, foldamers).[1] Oligomers of *N*-substituted glycine, or peptoids (Figure 1a),[2] are an important class of

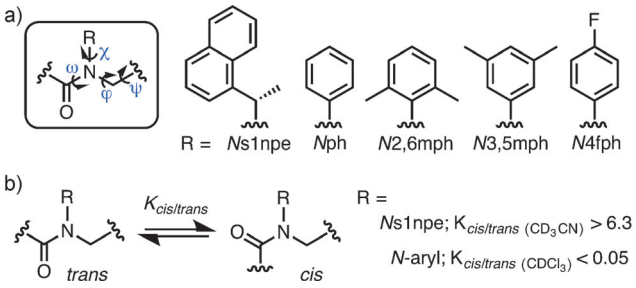

Figure 1. a) The primary structure of an α-peptoid oligomer (dihedral angles omega (ω), phi (ϕ), psi (ψ), and chi (χ) labeled) and the structures of the peptoid side chains discussed in this study. Side-chain abbreviations: s1npe = (*S*)-1-(1-naphthyl)ethyl; ph = phenyl; 2,6 mph = 2,6-dimethylphenyl; 3,5 mph = 3,5-dimethylphenyl; 4fph = 4-fluorophenyl. b) Peptoid *cis* and *trans* amide rotamers and the isomeric preferences engendered by the two amide side chains investigated in this study in model peptoid monomer systems.

foldamers that have been shown to possess numerous biological functions[3] and could find use in a range of fundamental and applied contexts as bio-inspired materials.[4] Peptoids are highly attractive scaffolds for such purposes, as their non-native backbones are resistant to proteolytic degradation[5] and their straightforward, modular synthesis[6] enables the ready incorporation of a range of structurally diverse amide side chains.[7] However, the design and prediction of peptoid secondary or higher-order structure remains a major challenge, and few discrete structures have been characterized to date for acyclic peptoids.[8] This paucity of structure–function data limits the potential utility of peptoids, despite their many advantages.

Structural studies of peptoids have been largely thwarted by the intrinsic conformational flexibility of the peptoid backbone itself. This backbone contains C-α methylene units, lacks hydrogen bond donating atoms, and, perhaps most notably, is linked by tertiary amides that can be isoenergetic between *cis* and *trans* amide geometries (Figure 1b). We and others reasoned that the development of peptoid side chains capable of engendering a high degree of control over proximate main-chain amide geometries could facilitate the design of well-defined peptoid structures and expand our understanding of peptoid folding.[9] We recently designed and synthesized a range of peptoid model systems to test this hypothesis, and have identified several classes of amide side chains that favor *cis* or *trans* main-chain amides in peptoid oligomers, predominantly through steric and stereoelectronic effects. One such side chain is the α-chiral aromatic (*S*)-1-(1-naphthyl)ethyl (s1npe) group (Figure 1), which strongly favors *cis* amide bonds (*cis*/*trans* > 6.3:1) in peptoid model systems.[9c] Moreover, *N*s1npe homooligomers adopt polyproline type I (PPI)-like peptoid helices that contain exclusively *cis* amides in the peptoid main chain.[8e] In turn, we found that the *trans* amide peptoid rotamer is strongly enforced by *N*-aryl side chains (for example, *N*ph, *cis*/*trans* < 0.05:1; Figure 1), and homooligomers of these residues have been calculated to give rise to extended, polyproline type II (PPII)-like peptoid helices with all *trans* amides.[9b] These peptoid monomers are thus a set of building blocks with which to initiate a rational construction of new peptoid secondary structures. Herein, we report our first test of this modular design strategy for peptoids and our ensuing discovery of a new secondary structure containing an alternating sequence of aromatic residues that we designate as the "peptoid ribbon".

In view of the strong rotameric preferences enforced in *N*-aryl and *N*s1npe monomers, we hypothesized that linear peptoids containing an alternating sequence of these two residues would adopt a well-defined and novel secondary structure with a regular, alternating pattern of *trans* and *cis* main-chain amides. A recent X-ray crystallographic report of an *N*-aryl/*N*s1npe dimer by Kirshenbaum and co-workers showed that the *N*-aryl amide bond was *trans* and that the *N*s1npe amide bond was *cis*,[10] and served to support our design hypothesis. The only known α-peptide sequences that adopt a regular, alternating pattern of *trans*/*cis* backbone

[*] Dr. J. A. Crapster,[+] I. A. Guzei, Prof. Dr. H. E. Blackwell
Department of Chemistry, University of Wisconsin-Madison
1101 University Avenue, Madison, WI 53706-1322 (USA)
E-mail: blackwell@chem.wisc.edu

[+] Current address: Department of Chemical and Systems Biology, Stanford University School of Medicine
269 Campus Drive, Stanford, CA 94305-5174 (USA)

[**] Financial support from the NSF (CHE-0449959), ONR (N000140710255), Greater Milwaukee Foundation, and Burroughs Welcome Fund is gratefully acknowledged. Chemistry NMR facilities at UW-Madison are supported by the NIH (1 S10 RR13866-01) and the NSF (CHE-0342998 and CHE-9629688). The National Magnetic Resonance Facility at UW-Madison is supported in part by NIH grants P41RR02301 (BRTP/NCRR) and P41GM66326 (NIGMS). We thank Dr. Charles Fry for assistance with NMR spectroscopy, Dr. Milo Westler for assistance with AMBER calculations, Prof. Samuel Gellman for thoughtful discussions and the use of his laboratory's CD spectrometer, and Dr. Joseph Stringer for experimental guidance.

Supporting information for this article, including full details of peptoid syntheses and characterization data (NMR, computations, X-ray crystallography, CD), is available on the WWW under http://dx.doi.org/10.1002/anie.201208630.

amides are alternating L-/D-polyprolines,[11] but no formal secondary structure designation has been assigned to these peptides. We reasoned that a systematic study of short, alternating *N*ph/*N*s1npe peptoid oligomers of increasing size would allow us to test our design premise.

We began our investigations by evaluating whether the *cis* or *trans* amide preferences of the *N*s1npe and *N*ph residues in solution were affected by being adjacent to each other in a heteropeptoid sequence, or by being placed at either the N- or C-terminal positions. Two dipeptoids, **2** and **2′** (Table 1), were synthesized by standard solution-phase methods (see the Supporting Information for full synthetic details),[9a,12] purified, and evaluated by NMR spectroscopy. Each peptoid was capped at the N-terminus with an acetyl group (Ac) and at the C-terminus as a dimethyl amide (dma) to 1) mimic the chemical environment of an extended peptoid chain at both termini; and 2) facilitate conformational analysis by ^{1}H–^{1}H nuclear Overhauser effect spectroscopy (NOESY). As expected, in CD_3CN at 24 °C, the $K_{cis/trans}$ values for the *N*s1npe residues in **2** and **2′** were 8.7 and 10.2, respectively, while the $K_{cis/trans}$ values for the *N*ph residues were 0.1 and 0.05, respectively. We note that the overall amide $K_{cis/trans}$ for homo dimers of *N*s1npe and *N*ph in CD_3CN were previously shown to be 10.8[8e] and <0.1,[9b] respectively, suggesting that their presence in heterodimers **2** and **2′** did not impact the rotameric preference of the other residue. The *cis* or *trans* amide preferences of the *N*s1npe and *N*ph residues in **2** and **2′** were also maintained in a variety of solvents ($CDCl_3$ (Table 1); C_6D_6, CD_3OD, [D_6]DMSO, and 1:1 CD_3CN/D_2O; Supporting Information, Table S1).

Table 1: Sequences, purities, mass spectrometry data, and overall *N*s1npe $K_{cis/trans}$ values for the peptoids investigated herein.

Peptoid	Sequence[a]	Purity [%][b]	Calcd mass	Obs. mass (m/z; $[M+Na]^+$)[c]	Overall $K_{cis/trans}$ values for *N*s1npe residues (in $CDCl_3$)
2	Ac-*N*ph-*N*s1npe-dma	>98	431.2	454.2	5[d]
2′	Ac-*N*s1npe-*N*ph-dma	>98	431.2	454.2	5[d]
3	Ac-*N*s1npe-*N*ph-*N*s1npe-dma	>98	642.3	665.3	10[e]
4a	Ac-*N*2,6 mph-*N*s1npe-*N*ph-*N*s1npe-dma	>98	803.4	826.4	25[e]
4b	Ac-*N*3,5 mph-*N*s1npe-*N*ph-*N*s1npe-dma	>98	803.4	826.4	19[e]
5	Ac-*N*s1npe-(*N*ph-*N*s1npe)$_2$-dma	>98	986.5	1009.5	47[e]
6	Ac-(*N*ph-*N*s1npe)$_3$-dma	>98	1119.5	1142.5	30[e]
6*i*	Ac-*N*3,5 mph-*N*s1npe-*N*2,6 mph-ac^{13}C-*N*s1npe-*N*4fph-*N*s1npe-dma	>98	1195.6	1218.6	28[e]
7	Ac-*N*s1npe-(*N*ph-*N*s1npe)$_3$-dma	>98	1330.6	1353.6	48[e]
8	Ac-(*N*ph-*N*s1npe)$_4$-dma	>98	1463.7	1486.7	53[e]

[a] Ac = acetyl, dma = dimethyl amide; see Figure 1a for monomer abbreviations. [b] Determined by integration of an HPLC trace with UV detection at 220 nm. [c] Mass spectrometry data were acquired using high-resolution ESI techniques. [d] Determined by integrating rotamer-related peaks in ^{1}H NMR spectra (500 MHz, 10 mM). [e] Determined by integrating rotamer-related peaks of the *N*s1npe methine protons in ^{1}H–^{13}C HSQC spectra (700 MHz, peptoids between 4–10 mM). See the Supporting Information for full details of methods used.

We next designed a trimer through octamer series of alternating peptoids **3**–**8** (Table 1) to determine if *cis* or *trans* amide preferences were maintained in longer sequences. Each was synthesized in solution and purified to homogeneity by manual column chromatography. As an initial solution-phase study of these systems, we conducted heteronuclear single-quantum correlation (HSQC) NMR experiments to determine the overall $K_{cis/trans}$ value for the *N*s1npe residues of each heteropeptoid. We anticipated that the *N*-aryl residues would adopt nearly exclusively *trans*-amide conformations,[9b,d] and thus, the overall *N*s1npe-amide $K_{cis/trans}$ value would correlate with the degree of overall amide rotamer homogeneity of a given oligomer. These NMR experiments were straightforward, as the *N*s1npe side-chain α-methine groups that are oriented in the *cis* geometry are readily distinguishable from those in the *trans* geometry by ^{1}H–^{13}C HSQC.[8d] In $CDCl_3$ (ca. 5 mM, 24 °C), we observed an extremely high preference for *cis* main-chain *N*s1npe amides in peptoids **3**–**8** ($K_{cis/trans} = 10$–53; Table 1), which, in general, increased as the peptoid chain length increased. This trend correlates with that observed for homo-oligomers of *N*s1npe.[8e] Also similar to *N*s1npe homo-oligomers, there was a considerable temperature-dependent decrease in the overall *N*s1npe amide $K_{cis/trans}$ values of **8** with increasing temperatures, in both $CDCl_3$ and CD_3OD, (Supporting Information, Table S2), suggesting an inherent entropic pressure for multiple rotameric conformers.

Tetramers **4a** and **4b** (Table 1) were specifically chosen as models for more detailed conformational analysis by NMR. Spectra for the tetramers were well-dispersed, with each residue clearly distinguishable and one conformer predominating. We envisioned that upon adopting a discrete secondary structure with alternating *cis* and *trans* amide bonds, the i and $i+3$ side chains of **4a** and **4b** could be in close proximity, facilitating the observation of NOEs between substituents on an *N*-aryl side chain at the i position and protons of an *N*s1npe side chain at the $i+3$ position. Our hypothesis proved correct, and Figure 2a depicts the NOEs that we detected between the dimethyl groups on the i (*N*-aryl) residues and the $i+3$ (*N*s1npe) methine and methyl protons for **4a** and **4b** in $CDCl_3$ (10 mM, 24 °C; see the Supporting Information, Figures S6 and S7 for additional analysis).

The NMR data for **4a** and **4b** inspired our design of hexamer **6*i*** (Figure 2b), with the goal of determining its solution-phase structure by NMR. We incorporated the ^{13}C-labeled main-chain acetyl group into the third residue of **6*i*** for assignment purposes and the fluoro-substituted *N*4fph residue to provide dispersion of resonance peaks. NMR

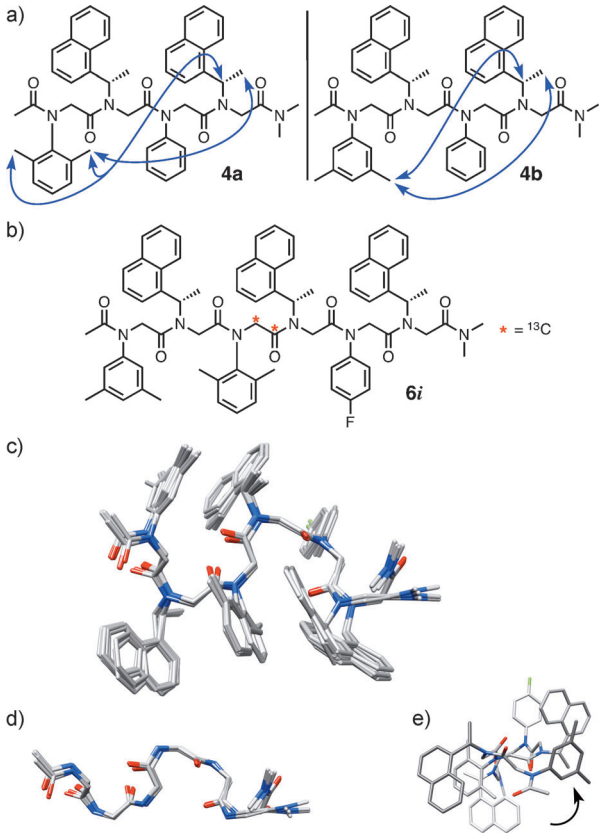

Figure 2. a) The structures of peptoid tetramers **4a** and **4b**; side-chain–side-chain NOEs are indicated with blue arrows. b) The structure of hexamer **6*i***. c) An ensemble of 10 superimposed low-energy structures of **6*i*** determined by NMR spectroscopy in $CDCl_3$ (hydrogen atoms are omitted for clarity). d) A length-wise view of the main-chain atoms of one population of low-energy structures of **6*i***. e) An axial view down the *N*-terminus of **6*i*** showing the left-handed spiral of the ribbon conformation.

spectra of hexamer **6*i*** were recorded in $CDCl_3$ (10 mM, 15 °C). One major conformer was observed in all NMR experiments and the resonances were well-dispersed, enabling the unambiguous assignment of main-chain methylenes, side-chain s1npe methines, and all methyl groups (Supporting Information, Figure S9 and Table S3). Rotating frame Overhauser effect spectroscopy (ROESY) cross-peaks were observed between i and $i+3$ side chains (residues 1↔4 and 2↔5), analogous to the NOEs observed in **4a** and **4b**. Unfortunately, ROE cross peaks between main-chain methylenes were not observed. However, the HSQC data described above provided evidence that each *N*s1npe amide in **6*i*** was primarily in the *cis* configuration. In total, nine distance restraints and three main-chain ω torsional restraints from our experimental NMR data were included in simulated annealing molecular dynamic calculations using AMBER11 software (see the Supporting Information for full details)[13] to determine an ensemble of calculated solution-phase structures for hexamer **6*i***.

The alignment of the 10 lowest energy structures for **6*i*** (out of 150 calculations) is shown in Figure 2c. These structures revealed a uniquely folded peptoid backbone of repeating turn units that resembled a ribbon-type structure. Two populations of low energy ribbon conformations were observed, with variation mainly at the C-terminus. In one population, the C-termini were extended in a continuation of the ribbon structure (Figure 2d; ensemble RMSD = 1.0 Å), while the C-termini of the second group of structures were curled inwards (ensemble RMSD = 1.1 Å; Supporting Information, Figure S10). Not including the C-termini, the mean ϕ and ψ values for the *N*s1npe residues in **6*i*** were −55° and 161°, respectively, and the mean ϕ and ψ values for the *N*aryl residues were 64° and −162°, respectively (see the Supporting Information, Table S4 for a full listing of ensemble-averaged main-chain dihedral angles). These values lie closest to the energetic minima calculated for peptoids in the α_D configuration (ϕ, $\psi = \pm 90°$, 180°), as defined by Moehle and Hofmann.[14] We also noted that the structure of **6*i*** clearly adopts a left-handed helical twist (Figure 2e). This characteristic has been observed in α-peptide ribbon structures, which are considered to be subtypes of helical peptide conformations (β-bend→3_{10}-helix).[15] We calculated the helical rotation between two hypothetical planes running through the two turn units in the hexamer ribbon. These planes were twisted by 34°; therefore, it would take 10.6 turn units (that is, $i-i+3$ sets of residues) to complete one full helical turn of the ribbon. Presumably, the origin of the left-handed spiral in **6*i*** is the chirality of the s1npe side chains.

Three heteropeptoids were crystalline upon slow evaporation from 1-propanol, and were further analyzed by X-ray crystallography. Solid-state structures for the synthetic intermediate Br-*N*ph-*N*s1npe-dma (representative of a peptoid dimer), trimer **3**, and tetramer **4a** are shown in Figure 3a, and allow the progressive generation of the ribbon secondary structure to be viewed as each residue is added. Tetramer **4a** is the shortest peptoid that is capable of adopting one full unit of the ribbon structure, and the reverse turn of the backbone approximates the i and $i+2$ main-chain methylene carbons of residues 1 and 3 (C···C distance = 4.97 Å; Figure 3b). Both **3** and **4a** adopted nearly identical conformations in the solid state, despite having different crystal packing interactions (Supporting Information, Figures S16, S18), which indicates that an alternating sequence of *N*s1npe and *N*-aryl residues can adopt a well-defined peptoid ribbon secondary structure even at short chain lengths. As expected, the amide geometries of all *N*s1npe residues were *cis* and all *N*-aryl residues were *trans*, and the ϕ and ψ angles of these solid state structures were in close agreement with the corresponding values determined for the NMR structure of hexamer **6*i*** (see the Supporting Information, Table S4 for a full listing of angles). This agreement is significant, as it constitutes the first corroboration of a peptoid NMR solution structure with peptoid solid-state structures containing the same primary sequences. The similarity is well illustrated by comparison of the solid state data and NMR data for **4a**. The X-ray crystal structure for **4a** shows that the methine proton of the $i+3$ *N*s1npe side chain is oriented directly towards a methyl group on the side chain of the *N*2,6mph (*i*) residue (C···C distance = 5.05 Å, Figure 3a). Accordingly, an NOE between the protons of these same groups was observed in our analysis of **4a** in $CDCl_3$ (see above).

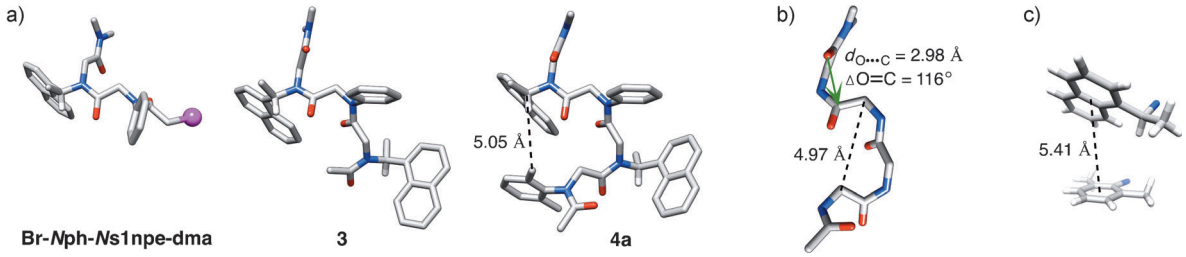

Figure 3. a) X-ray crystal structures of Br-Nph-Ns1npe-dma, **3**, and **4a**. All of the hydrogen atoms except for the s1npe side-chain methines have been omitted for clarity. The black dashed line indicates a side-chain–side-chain C···C distance. b) The main-chain atoms of the X-ray crystal structure of **4a** illustrate the reverse turn, and the green arrow depicts an $n\rightarrow\pi^*_{C=O}$ interaction. The black dashed line indicates a main chain Cα···Cα distance. c) A displaced aromatic–aromatic stacking interaction was detected between the side chains of residues 1 and 4 in the X-ray crystal structure of **4a**. Only the side-chain and nitrogen atoms are shown. The black dashed line indicates the centroid to centroid distance between the two aryl rings.

The solution phase and crystal structures were further analyzed for potential noncovalent interactions that may stabilize the peptoid ribbon conformation, which lacks a hydrogen bonding network. Interestingly, in all structures, every other backbone carbonyl was oriented perpendicular to one other, but the overall dipole was pointed towards the N-terminus. At the C-terminus of **4a**, we detected an $n\rightarrow\pi^*_{C=O}$ interaction (Figure 3b).[16] Previous X-ray crystallographic studies in our laboratory have revealed that $C{=}Oi-1\cdots C'i=O$ interactions can exist in peptoid monomers and at the N-terminus of a peptoid oligomer,[9a,d] yet this is, to our knowledge, the first report of an $C{=}Oi+1\cdots C'i=O$ interaction in peptoids. We analyzed all sequential backbone carbonyl groups in the structures of **3**, **4a**, and **6*i*** for $n\rightarrow\pi^*_{C=O}$ interactions, and although the distances between the main-chain carbonyl oxygen atoms and the carbonyl carbon atoms of the preceding or subsequent residue were under 3.2 Å (as is typical for the $n\rightarrow\pi^*$ interaction[16]), the angle of approach was outside of the $109\pm10°$ window necessary for sufficient orbital overlap in all but the C-terminal residue of **4a**.[17] We therefore surmise that $n\rightarrow\pi^*_{C=O}$ interactions do not play a major role in enforcing the ribbon conformation in these peptoids.

We also evaluated the structures of **4a** and **6*i*** for intramolecular aromatic–aromatic interactions between side chains by measuring the angles between the aryl planes, the distances between the aryl centroids, and the distances between nearest interresidue atoms.[18] In the X-ray crystal structure of **4a**, the i and $i+3$ side chains are positioned in an oblique orientation of a displaced stacking interaction (angle between aromatic planes = 33.5°) with a centroid–centroid distance of 5.4 Å and nearest interresidue C–C distance of 4.6 Å (Figure 3c; Supporting Information, Figure S11a). Correspondingly, the ensemble of NMR structures of **6*i*** also revealed displaced aromatic stacking interactions between the i and $i+3$ residues at the beginning and end of each turn unit (Supporting Information, Figure S11b–d). Elucidating the contribution, if any, of these aromatic–aromatic interactions to the thermodynamic stability of the peptoid ribbon is an important avenue for future study, and is the subject of ongoing investigations in our laboratory.

We next used circular dichroism (CD) spectroscopy to study the effects of peptoid length, solvent, and temperature on the ribbon structure. The CD spectra for all of the peptoid oligomers had nearly identical spectral features in acetonitrile, 1:1 acetonitrile/water, and methanol (negative maxima of ellipticity at 224–226 nm and broad positive peaks of ellipticity between 197–205 nm; Figure 4), indicating that all of the peptoids in this series adopted similar secondary structures in both organic and polar protic solvents (at 30 μM, 20 °C). Additionally, CD data for peptoid **8** at varying concentrations (7–80 μM) in acetonitrile suggested that intermolecular interactions were not affecting the observed CD signal (Supporting Information, Figure S19). Interestingly, the CD spectra of the peptoid ribbon most closely resembled data reported for poly-LD-Pro sequences,[19] which also adopt an alternating *cis*/*trans* amide backbone pattern. Beyond the dimer chain length, there were no length-dependent changes in the CD spectral intensities. Instead, in all solvents, we observed a difference in signal intensity between even and odd numbered chain lengths. This effect could potentially be due to the absorption properties of the s1npe side chains, which are more solvent-exposed in the ribbon as the C-terminal residue in odd numbered chain lengths.

The CD spectral shape for peptoids **2**–**8** varied slightly in the different solvents. In the acetonitrile/water mixture, shoulders were apparent in all CD traces from 227–230 nm (Figure 4b), and the shoulders were more pronounced in methanol (Figure 4c). These observations could indicate a slight change in overall conformation that is solvent-dependent, or a change in the UV adsorption properties or orientations of the aromatic side chains in these solvents. Lastly, the thermal stability of **8** (30 μM) was examined in acetonitrile (15–75 °C), 1:1 acetonitrile/water (10–75 °C), and methanol (10–65 °C) (Supporting Information, Figures S20–S22). A linear decrease in signal intensity was observed with increasing temperatures; however, the spectral shape of **8** in all solvents was maintained throughout the temperature ranges investigated. This temperature destabilization can be attributed, in part, to the increase in amide bond isomerization at elevated temperatures that we observed in ^1H–^{13}C HSQC experiments for **8** (see above).

In summary, we report a new peptoid secondary structure comprised of a regular alternating sequence of *N*s1npe and *N*-aryl residues, which we term the "peptoid ribbon". This structure is a result of our first rational design of discretely

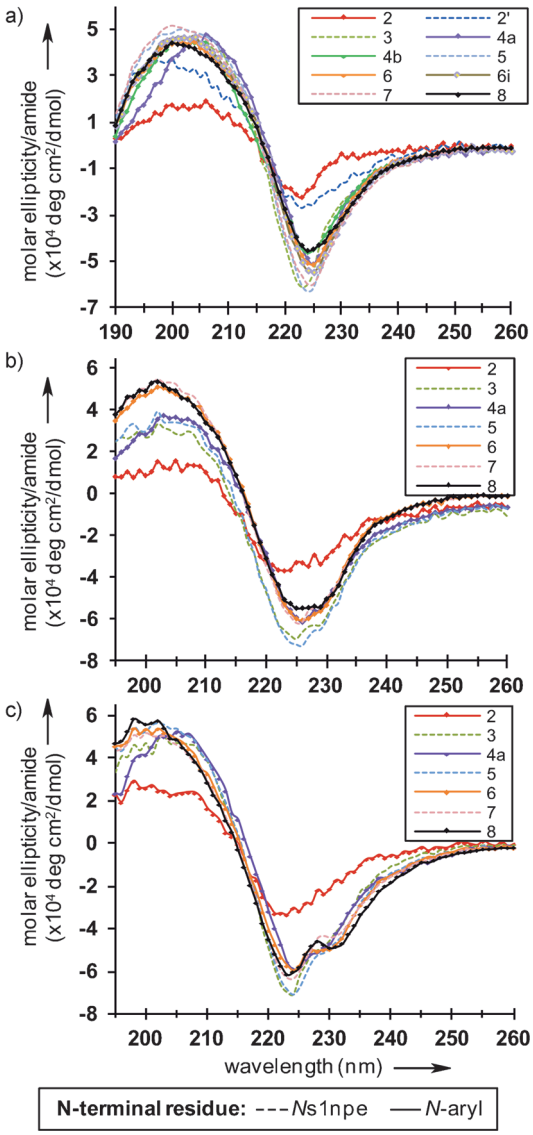

Figure 4. CD spectra of a) all peptoids in acetonitrile, b) selected peptoids in a 1:1 acetonitrile/water mixture, and c) selected peptoids in methanol. All of the spectra were obtained at 30 μM and 20 °C.

folded peptoids using monomers with defined amide rotamer preferences. Systematic NMR, X-ray crystallographic, and CD studies of a series of *N*s1npe/*N*ph heteropeptiods revealed that the ribbon is stable at short chain lengths and in both protic and aprotic solvents. Perhaps most notably, we present corroborating solution-phase NMR and solid-state structures for ribbons with the same primary sequence, a level of structural characterization yet to be achieved for other peptoid secondary structures. The peptoid ribbon can be described as a succession of turn units that is similar in appearance to known LD-ribbon[15] and β-bend ribbon[20] folds in α-peptides. However, in the latter ribbon structures, all main-chain amide bonds are in the *trans* configuration. The alternating *cis*/*trans* geometry of the main-chain amides and the preclusion of hydrogen bonds within the peptoid backbone gives rise to a secondary structure that is, to the best of our knowledge, wholly unique to these peptoids. The steric demands of the bulky, chiral s1npe side chain undoubtedly play a dominant role in facilitating the ribbon conformation and enforcing the left-handed spiral of the peptoid ribbon. Small model systems have proven to be powerful for understanding the processes by which foldamers and natural biopolymers fold.[1a,b,21] The discovery of a peptoid ribbon secondary structure underscores the value of such model systems for peptoid design. Looking forward, we note that several classes of α-peptide ribbons are known to act as potent and selective antibiotics[22] and cell-membrane-modifying agents.[23] Helical and cyclic peptoids have previously been investigated for similar functions,[24] and the peptoid ribbon could now be considered for such applications, among others.

Received: October 26, 2012
Revised: January 2, 2013
Published online: April 9, 2013

Keywords: foldamers · peptidomimetics · peptoids · ribbons · secondary structure

[1] a) S. H. Gellman, *Acc. Chem. Res.* **1998**, *31*, 173–180; b) C. M. Goodman, S. Choi, S. Shandler, W. F. DeGrado, *Nat. Chem. Biol.* **2007**, *3*, 252–262; c) S. A. Fowler, H. E. Blackwell, *Org. Biomol. Chem.* **2009**, *7*, 1508–1524.

[2] R. J. Simon, et al., *Proc. Natl. Acad. Sci. USA* **1992**, *89*, 9367–9371 (see the Supporting Information for all authors).

[3] a) R. N. Zuckermann, T. Kodadek, *Curr. Opin. Mol. Ther.* **2009**, *11*, 299–307; b) W. S. Horne, *Expert Opin. Drug Discov.* **2011**, *6*, 1247–1262; c) V. Kesavan, N. Tamilarasu, H. Cao, T. M. Rana, *Bioconjugate Chem.* **2002**, *13*, 1171–1175; d) L. S. Simpson, L. Burdine, A. K. Dutta, A. P. Feranchak, T. Kodadek, *J. Am. Chem. Soc.* **2009**, *131*, 5760–5762; e) J. Lee, D. G. Udugamasooriya, H.-S. Lim, T. Kodadek, *Nat. Chem. Biol.* **2010**, *6*, 258–260; f) M. M. Reddy, R. Wilson, J. Wilson, S. Connell, A. Gocke, L. Hynan, D. German, T. Kodadek, *Cell* **2011**, *144*, 132–142; g) X. Chen, J. Wu, Y. Luo, X. Liang, C. Supnet, M. W. Kim, G. P. Lotz, G. Yang, P. J. Muchowski, T. Kodadek, I. Bezprozvanny, *Chem. Biol.* **2011**, *18*, 1113–1125.

[4] a) H. K. Murnen, A. M. Rosales, J. N. Jaworski, R. A. Segalman, R. N. Zuckermann, *J. Am. Chem. Soc.* **2010**, *132*, 16112–16119; b) K. T. Nam, S. A. Shelby, P. H. Choi, A. B. Marciel, R. Chen, L. Tan, T. K. Chu, R. A. Mesch, B.-C. Lee, M. D. Connolly, C. Kisielowski, R. N. Zuckermann, *Nat. Mater.* **2010**, *9*, 454–460; c) L. Guo, D. Zhang, *J. Am. Chem. Soc.* **2009**, *131*, 18072–18074; d) C. Fetsch, A. Grossmann, L. Holz, J. F. Nawroth, R. Luxenhofer, *Macromolecules* **2011**, *44*, 6746–6758.

[5] a) S. M. Miller, R. J. Simon, S. Ng, R. N. Zuckermann, J. M. Kerr, W. H. Moos, *Bioorg. Med. Chem. Lett.* **1994**, *4*, 2657–2662; b) S. M. Miller, R. J. Simon, S. Ng, R. N. Zuckermann, J. M. Kerr, W. H. Moos, *Drug Dev. Res.* **1995**, *35*, 20–32.

[6] a) R. N. Zuckermann, J. M. Kerr, S. B. H. Kent, W. H. Moos, *J. Am. Chem. Soc.* **1992**, *114*, 10646–10647; b) B. C. Gorske, S. A. Jewell, E. J. Guerard, H. E. Blackwell, *Org. Lett.* **2005**, *7*, 1521–1524.

[7] a) B. Yoo, K. Kirshenbaum, *Curr. Opin. Chem. Biol.* **2008**, *12*, 714–721; b) A. S. Culf, R. J. Ouellette, *Molecules* **2010**, *15*, 5282–5335.

[8] a) P. Armand, K. Kirshenbaum, A. Falicov, R. L. Dunbrack, Jr., K. A. Dill, R. N. Zuckermann, F. E. Cohen, *Folding Des.* **1997**, *2*, 369–375; b) P. Armand, K. Kirshenbaum, R. A. Goldsmith, S. Farr-Jones, A. E. Barron, K. T. V. Truong, K. A. Dill, D. F.

Mierke, F. E. Cohen, R. N. Zuckermann, E. K. Bradley, *Proc. Natl. Acad. Sci. USA* **1998**, *95*, 4309 – 4314; c) C. W. Wu, K. Kirshenbaum, T. J. Sanborn, J. A. Patch, K. Huang, K. A. Dill, R. N. Zuckermann, A. E. Barron, *J. Am. Chem. Soc.* **2003**, *125*, 13525 – 13530; d) K. Huang, C. W. Wu, T. J. Sanborn, J. A. Patch, K. Kirshenbaum, R. N. Zuckermann, A. E. Barron, I. Radhakrishnan, *J. Am. Chem. Soc.* **2006**, *128*, 1733 – 1738; e) J. R. Stringer, J. A. Crapster, I. A. Guzei, H. E. Blackwell, *J. Am. Chem. Soc.* **2011**, *133*, 15559 – 15567.

[9] a) B. C. Gorske, B. L. Bastian, G. D. Geske, H. E. Blackwell, *J. Am. Chem. Soc.* **2007**, *129*, 8928 – 8929; b) N. H. Shah, G. L. Butterfoss, K. Nguyen, B. Yoo, R. Bonneau, D. L. Rabenstein, K. Kirshenbaum, *J. Am. Chem. Soc.* **2008**, *130*, 16622 – 16632; c) B. C. Gorske, J. R. Stringer, B. L. Bastian, S. A. Fowler, H. E. Blackwell, *J. Am. Chem. Soc.* **2009**, *131*, 16555 – 16567; d) J. R. Stringer, J. A. Crapster, I. A. Guzei, H. E. Blackwell, *J. Org. Chem.* **2010**, *75*, 6068 – 6078; e) J. A. Crapster, J. R. Stringer, I. A. Guzei, H. E. Blackwell, *Pept. Sci.* **2011**, *96*, 604 – 614; f) P. A. Jordan, B. Paul, G. L. Butterfoss, P. D. Renfrew, R. Bonneau, K. Kirshenbaum, *Biopolymers* **2011**, *96*, 617 – 626; g) C. Caumes, O. Roy, S. Faure, C. Taillefumier, *J. Am. Chem. Soc.* **2012**, *134*, 9553 – 9556.

[10] B. Paul, G. L. Butterfoss, M. G. Boswell, M. L. Huang, R. Bonneau, C. Wolf, K. Kirshenbaum, *Org. Lett.* **2012**, *14*, 926 – 929.

[11] a) E. Benedetti, A. Bavoso, B. Diblasio, V. Pavone, C. Pedone, C. Toniolo, G. M. Bonora, *Biopolymers* **1983**, *22*, 305 – 317; b) M. Colapietro, P. Desantis, A. Palleschi, R. Spagna, *Biopolymers* **1986**, *25*, 2227 – 2236.

[12] T. Hjelmgaard, S. Faure, C. Caumes, E. De Santis, A. A. Edwards, C. Taillefumier, *Org. Lett.* **2009**, *11*, 4100 – 4103.

[13] D. A. Case, et al., *AMBER 11*, University of California, San Francisco, **2010** (see the Supporting Information for all authors).

[14] K. Moehle, H.-J. Hofmann, *Biopolymers* **1996**, *38*, 781 – 790.

[15] R. Chandrasekaran, B. V. V. Prasad, *Crit. Rev. Biochem. Mol. Biol.* **1978**, *5*, 125 – 161.

[16] A. Choudhary, D. Gandla, G. R. Krow, R. T. Raines, *J. Am. Chem. Soc.* **2009**, *131*, 7244 – 7246.

[17] a) H. B. Burgi, J. D. Dunitz, E. Shefter, *J. Am. Chem. Soc.* **1973**, *95*, 5065 – 5067; b) H. B. Burgi, J. D. Dunitz, J. M. Lehn, G. Wipff, *Tetrahedron* **1974**, *30*, 1563 – 1572.

[18] a) T. Blundell, J. Singh, J. Thornton, S. K. Burley, G. A. Petsko, *Science* **1986**, *234*, 1005; b) L. Brocchieri, S. Karlin, *Proc. Natl. Acad. Sci. USA* **1994**, *91*, 9297 – 9301; c) G. B. McGaughey, M. Gagné, A. K. Rappé, *J. Biol. Chem.* **1998**, *273*, 15458 – 15463.

[19] W. Mastle, R. K. Dukor, G. Yoder, T. A. Keiderling, *Biopolymers* **1995**, *36*, 623 – 631.

[20] a) Y. V. Venkatachalapathi, P. Balaram, *Biopolymers* **1981**, *20*, 1137 – 1145; b) I. L. Karle, J. Flippenanderson, M. Sukumar, P. Balaram, *Proc. Natl. Acad. Sci. USA* **1987**, *84*, 5087 – 5091.

[21] K. A. Dill, *Biochemistry* **1990**, *29*, 7133 – 7155.

[22] A. D. Argoudelis, A. Dietz, L. E. Johnson, *J. Antibiot.* **1974**, *27*, 321 – 328.

[23] P. De Santis, A. Palleschi, M. Savino, A. Scipioni, B. Sesta, A. Verdini, *Biophys. Chem.* **1985**, *21*, 211 – 215.

[24] a) N. P. Chongsiriwatana, J. A. Patch, A. M. Czyzewski, M. T. Dohm, A. Ivankin, D. Gidalevitz, R. N. Zuckermann, A. E. Barron, *Proc. Natl. Acad. Sci. USA* **2008**, *105*, 2794 – 2799; b) M. L. Huang, S. B. Y. Shin, M. A. Benson, V. J. Torres, K. Kirshenbaum, *ChemMedChem* **2012**, *7*, 114 – 122.

